

# Energy-Efficient Low-Temperature Heat Pump Drying of Mint Leaves: Preserving Quality and Energy

Sachin R. Shinde<sup>1,\*</sup>, Bhaskar N. Thorat<sup>2</sup>, Suresh P. Deshmukh<sup>1</sup>

<sup>1</sup>Department of General Engineering, Institute of Chemical Technology, Mumbai, India

<sup>2</sup>Department of Chemical Engineering, Institute of Chemical Technology, Mumbai, India

Received April 7, 2025; Revised June 9, 2025; Accepted July 16, 2025

## Cite This Paper in the Following Citation Styles

(a): [1] Sachin R. Shinde, Bhaskar N. Thorat, Suresh P. Deshmukh, "Energy-Efficient Low-Temperature Heat Pump Drying of Mint Leaves: Preserving Quality and Energy," *Food Science and Technology*, Vol. 13, No. 3, pp. 261 - 273, 2025. DOI: 10.13189/fst.2025.130303.

(b): Sachin R. Shinde, Bhaskar N. Thorat, Suresh P. Deshmukh (2025). *Energy-Efficient Low-Temperature Heat Pump Drying of Mint Leaves: Preserving Quality and Energy*. *Food Science and Technology*, 13(3), 261 - 273. DOI: 10.13189/fst.2025.130303.

Copyright©2025 by authors, all rights reserved. Authors agree that this article remains permanently open access under the terms of the Creative Commons Attribution License 4.0 International License

**Abstract** High-temperature drying can damage heat-sensitive materials if dried directly by heaters, sun drying, or heat pumps operating at 40°C to 90°C, causing loss of fragrance and colour. Vacuum and freeze-drying are common low-temperature methods, but they're expensive and slow that limits their uses. A more efficient alternative is low-temperature heat pump drying. This research concentrates on designing and developing energy-efficient low-temperature heat pump drying system for heat-sensitive materials. Present paper provides two-stage heat pump drying system that works below 35 °C, producing high-quality dried products. The paper focuses on designing, dimensioning, and operating a low-temperature heat pump dryer. Drying properties of mint leaves are also analyzed at 2, 2.5, and 3 m/s air velocities and low temperatures from 30-40°C. The system performance includes heating load, power consumption, coefficient of performance, specific moisture extraction rate (SMER) etc. Average coefficient of performance (COP) achieved was 4.8, with average SMER being 0.84 kg/kW-hr. Experimental results demonstrate system's ability to preserve quality in addition to properties of heat-sensitive materials. These results hold important relevance for industries such as pharmaceuticals, food processing, and biotechnology, where maintaining integrity of products is essential. This study advances drying technology by introducing an innovative approach for drying heat-sensitive materials that reduces energy usage while maintaining quality. The proposed system presents a viable alternative to traditional drying

techniques, especially in sectors where both product quality and energy savings are critical. By providing a consistent airflow at controlled sub-zero temperatures, the system eliminates reliance on external heating for defrosting, thereby improving overall energy efficiency.

**Keywords** Coefficient of Performance, Heat Rejection Rate, Heat Sensitive Materials, Low-Temperature Heat Pump Drying, Specific Moisture Extraction Rate

---

## 1. Introduction

Drying is time-consuming as well as energy-intensive process [1]. Most agricultural products, such as wood, food, paper and pulp, rubber, pharmaceuticals, etc., need drying to avoid spoilage and wastage and to lower transportation costs [2]. In this paper, drying characteristics of mint leaves are analyzed. If product is heat-sensitive, hot air drying isn't considered a suitable method as it can impact the colors, texture, fragrance, etc. Vacuum drying is a good choice for such products. Other alternatives, like indirect-type solar passive drying, are also available for drying mint leaves [3], [4]. Solar drying is not continuous and cannot be operated at controlled parameters. Microwave drying speeds up the drying process; however, it can cause a reduction in the brightness and green color of vegetables. Ertekin et al. [5] used temperature of 60-70 °C in infrared dryers for drying mint leaves, and they found

that drying time was significantly decreased if dried at high temperatures. Still, the yellowness of dried mint also rose, as compared to the fresh mint leaves sample.

Many researchers have focused on different drying technologies that involve designing and developing heating, air circulating, and dehumidification units and using other methods like infrared, convective, and microwave drying[6], [7], [8]. Amongst all the techniques used for drying mints, heat pump dryer (HPD) is the most advanced and energy-efficient system, as it provides higher thermal output than compared to electrical input supplied to operate it[9], [10]. It provides dehumidified air at both high and low temperatures. The low-temperature dehumidified air is ideal for drying heat-sensitive materials in a controlled atmosphere [11], [12]. Several studies have been conducted on HPD with low supply temperature as well as low relative humidity (RH) in drying chamber [13], [14]. For achieving higher efficiency of such dryers, many researchers have used multistage throttling, series, or parallel combinations of evaporators. According to Invernizzi and Angelin [15], the simple heat pump cycle can achieve better performance by enabling more heat recovery through multistage throttling and compression processes. Praphanpong et al.[16] reported that adding external condensers for heat recovery is more efficient way compared to traditional heat pump systems. Chua et al. [17] conducted experiments on the two-stage heat pump drying system with 2 evaporators arranged in parallel integration and reported around 35% more heat recovered via two stages. In contrast, Chao-Jen Li et al. [18] reported that two evaporators in a series can save the energy of heat pump cycle. Anran Du et al. [19] analyzed heating performance of heat pump system using two-stage evaporator for drying applications. The purpose of using a double evaporator system is to provide a larger heat transfer surface, thus improving the system's performance from a thermodynamic point of view[20].

The degree of dehumidification can be effectively lowered by lowering the process air temperature below zero degrees. Such air with low absolute humidity will have a very low vapor pressure. This air with very low vapor pressure creates the driving force while drying heat-sensitive material at low temperatures. So far, the reported two-stage heat pump systems do not operate at sub-zero temperatures (dew point at saturation and dry bulb temperature subsequently) without being affected by the defrosting cycle.

In this study, an experimental investigation was conducted on production of an energy-efficient heat pump drying system which can supply a continuous stream of low-humidity air at near-ambient temperatures, with a corresponding water vapor pressure of approximately 420Pa. The system achieves deep dehumidification by removing the majority of moisture from the incoming air, thereby generating air with low absolute humidity, which is

introduced into the drying chamber at atmospheric pressure and temperature. This low vapor pressure environment facilitates moisture migration from within the material, driven by the internal vapor pressure gradient and governed by the material's effective diffusivity. The dehumidification process is carried out at a dew point several degrees below 0 °C, and is uninterrupted by defrost cycles due to use of a parallel heat pump configuration. Dehumidified air is subsequently reheated to near-ambient temperatures using waste heat recovered from the compressor's superheater and condenser sub-cooler stages, enhancing overall thermal efficiency. Dryer comprises air-to-air heat recovery unit, air-source heat pump system, along with proportional temperature controllers. The ability to dehumidify air without interruption from a defrost cycle and provide continuous flow of dry air at ambient temperature and low vapor pressure is a unique aspect of current paper.

## 2. Materials and Methods

### 2.1. Experimental Setup

The prototype comprises a compressor, a condenser, 2 evaporator sets, an expansion valve, a back pressure-reducing valve, a fan controller, sensors, along with drying cabinet. Details of drying system are displayed in **Figure 1**.

The drying system is demonstrated in **Figure 2**. Heat pumps and drying chambers are designed to satisfy two main goals: to cool down the air over high-pressure and low-pressure evaporators separately. By cooling air in two stages, the system can eliminate more moisture from air, resulting in lower humidity levels. With two evaporators, the system can maintain a more stable temperature, reducing temperature fluctuations and improving overall system performance. The system also reduces the likelihood of frosting on the evaporator coils, which can decrease system performance and increase maintenance needs[21]. The high-pressure evaporator (HPE) system is shown by Paths 1-6, whereas the low-pressure evaporator (LPE) system is demonstrated by Paths 7-13. For the full-scale capacity, one direct-expansion evaporator of 1-tonne cooling capacity employed in a high-pressure system and two direct-expansion evaporators (each evaporator is of half of cooling capacity of high-pressure evaporator, i.e., half tonne each) in a low-pressure evaporator system are selected. The evaporators were arranged on the air path to remove the sensible heat separately at HPE. In contrast, latent heat was released at LPEs, consequently, bringing the air temperature below sub-zero and obtaining effective air dehumidification after the evaporator chamber. The solenoid valve controls liquid refrigerant flowing into the LPE coils for dehumidification.

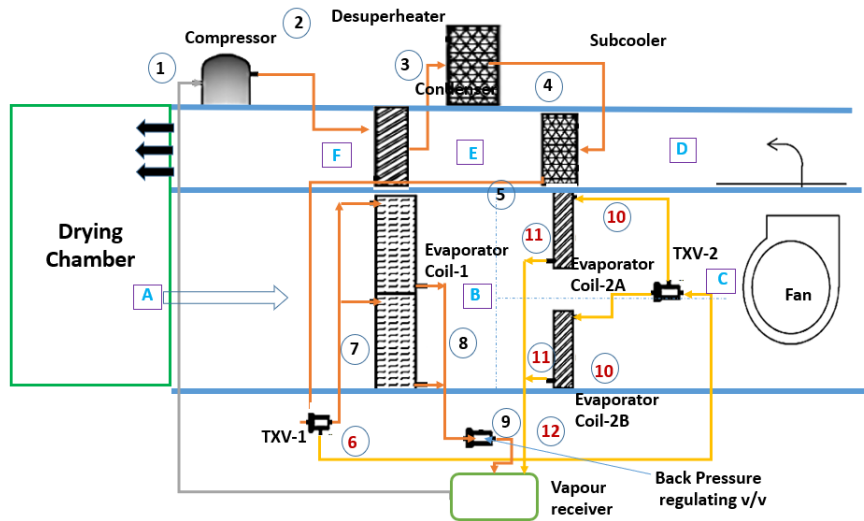


Figure 1. Concept Diagram

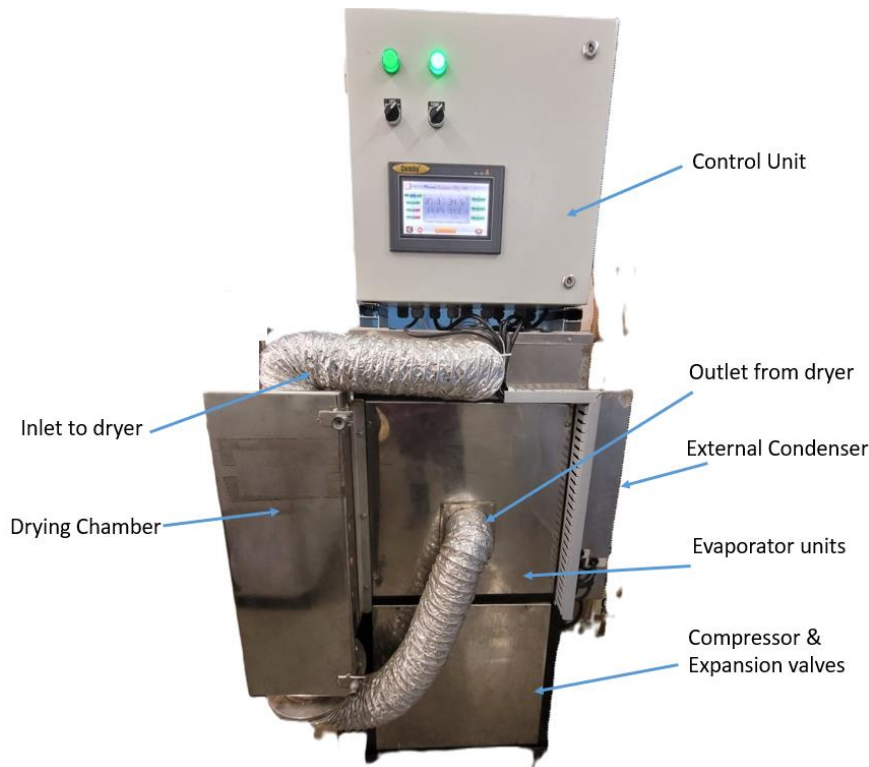


Figure 2. The drying system prototype

Second, a separate sub-cooler and desuperheater are arranged on an air path. The air temperature can be significantly increased if external condensers are used on the way of the air stream. As system is designed for low-temperature heat pump drying applications, only sensible heat from the sub-cooler and desuperheater was taken to raise temperature of dry air. Solenoid valves modulate cooling fan operation of the external condenser, thereby regulating the sub-cooler's temperature in response to dry air supply temperature requirements. To achieve a higher temperature setpoint, the solenoid valves reduce the fan speed, allowing the external condenser to reject heat to

the ambient environment. Consequently, the sub-cooler's capacity to transfer heat to the process air increases. Furthermore, an air bypass is incorporated downstream of the desuperheater to regulate the dry air flow rate entering the drying chamber. This bypass ensures a consistent airflow rate throughout the system, thereby maintaining optimal drying conditions. The system's design facilitates precise temperature control, airflow regulation, efficient heat transfer, and a stable drying environment. The components are designed and fabricated by considering the 1-tonne capacity of each evaporator. Equipment and its technical specifications are shown in **Table 1**.

**Table 1.** List of Components

Equipment	Description	Type and Dimension
<b>Low-Pressure Evaporator</b>	Face area	0.0775 m <sup>2</sup>
	Fin pitch	4 mm
	Number of tube columns	4
	Number of tube rows	5
	Quantity	2
<b>High-Pressure Evaporator</b>	Face area	0.155 m <sup>2</sup>
	Fin pitch	4 mm
	Number of tube columns	4
	Number of tube rows	5
	Quantity	1
<b>Subcooler</b>	Face area	0.075 m <sup>2</sup>
	Fin pitch	4 mm
	Number of tube columns	3
	Number of tube rows	4
	Quantity	2
<b>Condenser</b>	Face area	0.155 m <sup>2</sup>
	Fin pitch	4 mm
	Number of tube columns	4
	Number of tube rows	5
	Quantity	2
<b>Desuperheater</b>	Face area	0.0775 m <sup>2</sup>
	Fin pitch	4 mm
	Number of tube columns	3
	Number of tube rows	4
	Quantity	2
<b>Expansion valve</b>	Make	Danfoss TE2X2-2.3
	Quantity	2
<b>Compressor</b>	Make and Model	KCJ513HAE 5420H
<b>Pressure reducing Valve</b>	Danfoss KVP 15 022	1
<b>Refrigerant</b>	R410A	
<b>Air volume flow rate in the drying chamber</b>	0.0472 m <sup>3</sup> /s	
<b>Air volume flow rate across evaporators</b>	0.188-0.288 m <sup>3</sup> /s	
<b>Supply air velocity</b>	2-3 m/s	

## 2.2. Experimental Procedure

Air enters from the dryer to the HPE, cooled to around 4 °C. This cooled air is divided into two halves, where half of the air quantity moves onto the LPE-1 and the remaining half flows over the LPE-2. The cold air is dehumidified below zero degrees Centigrade in both the LPEs. While cooling the air below zero degrees Centigrade, an ice formation on the evaporator coils is observed. Defrosting is done by pulsing hot refrigerant gas from the compressor's outlet for a few seconds into the evaporator coils. The minimum temperature at which defrosting is activated is set at both LPEs. If the air temperature falls below the set value, the defrosting starts. Using two LPEs in parallel allows for continuous defrosting without disrupting the air cycle, ensuring a consistent supply of dehumidified air. A

timer in the control panel controls the defrosting so that ice does not have time to form on the coil having sub-zero temperatures. Air dampers are provided on the air path while defrosting is carried out so that moisture doesn't mix with the final dehumidified air. The use of air dampers to prevent moisture from mixing with the dehumidified air during defrosting maintains the air's low vapor pressure. **Figure 3** shows the arrangement of defrosting and air on the HP and LP evaporator coils. The hot gas from compressor discharge line pulses into evaporator coil for a few seconds. As soon as defrosting is completed, this pulsing of hot gas stops. The temperature sensor is set on the evaporator coils to ensure the completion of the defrosting process. This defrosting arrangement is made on both of the low-pressure evaporators. This arrangement of

LPEs ensures that the air cycle is not disturbed due to the defrosting stage, and a continuous supply of air with sub-zero temperatures is maintained. The air streams from two LPEs mixes and goes over the sub-cooler. Defrosting is achieved by pulsing hot refrigerant gas from compressor discharge line into evaporator coils, which is an efficient and effective method. The dehumidified cold air obtained from the LPEs has very low vapor pressure. This dehumidified air is heated along the path by the desuperheater and sub-cooler to desired temperature. This low-temperature dehumidified air is then transferred into the drying chamber.

The air continuously flows through the closed system. The bypass air is removed from the desuperheater exit and

supplied back to the entry of high-pressure evaporators. Suitable dampers are provided to divert the airflow and are controlled manually. Dampers are also provided at the entrance of LPEs. When the air passes on the LPE-1, the dampers close the air path on LPE-2. The airflow path is shown in **Figure 4**.

A digital balance was employed to monitor the moisture loss from the mint leaves during drying. Temperature readings were taken using a K-type thermocouple. Air conditions entering drying chamber, including temperature and relative humidity, were regulated through an electronic control panel.

**Table 2** shows the various measuring devices used for measuring air quantities and refrigerant properties.

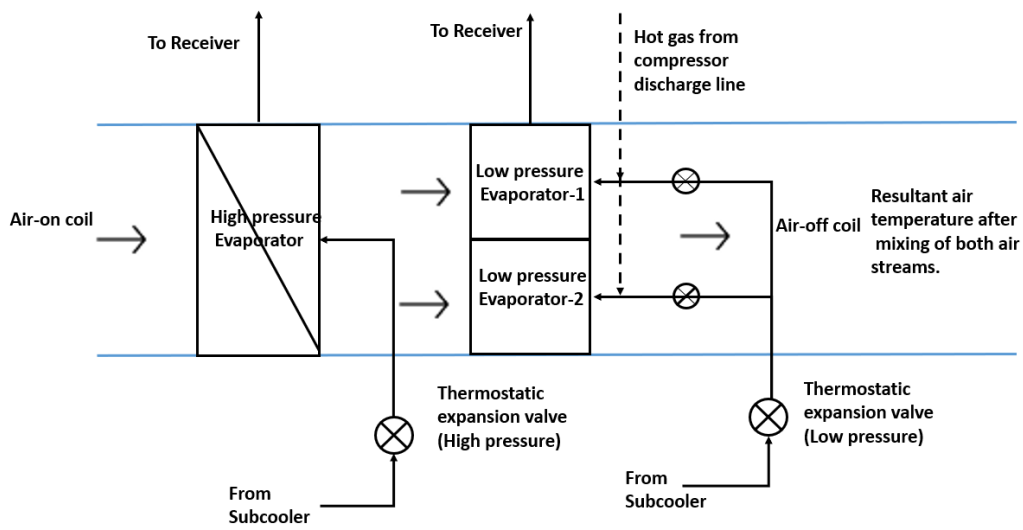


Figure 3. Defrosting arrangement

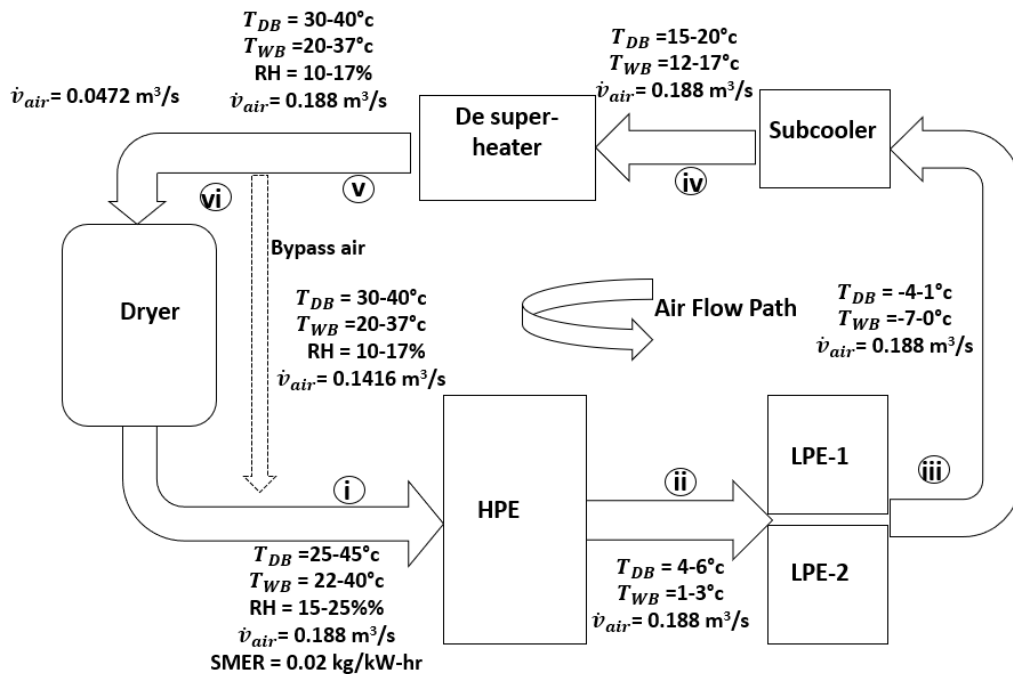
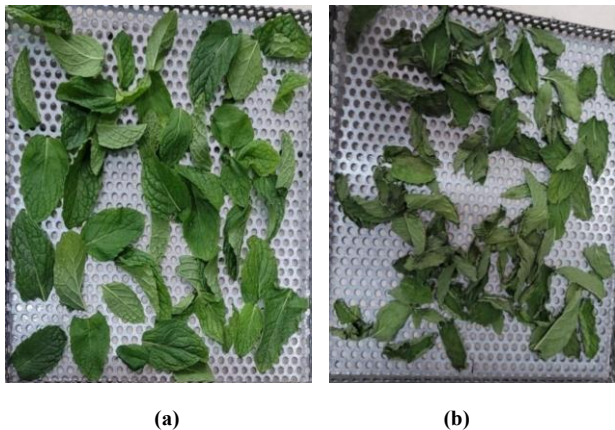


Figure 4. Airflow Path

**Table 2.** Measuring devices and their uncertainties

Measuring sensor	Measured Property	Range	Uncertainty
Power clamp-on meter	Compressor power input	0-10kW	±0.5%
Pressure transducer gauges	Inlet and Outlet Refrigerant temperature	50-500psi	±0.5%
Resistive Temperature Detector	Inlet and Outlet Refrigerant temperature	-10 to 90 °C.	±2%
Rh sensor	Inlet and Outlet air humidity	5-97%	±1.0%
Type "T" Thermocouple	Inlet and outlet air temperatures	2- 95 °C.	±2.5%

Mint leaves' dry weight was measured by placing samples in hot air oven at  $100 \pm 1$  °C under atmospheric conditions. 100g fresh mint leaves were selected for each trial. Drying was performed at temperatures selected to preserve natural enzymatic activity and minimize degradation during storage, hence conditions were maintained near ambient levels. The leaves were arranged on trays, and drying trials were conducted at three distinct air velocities: 2, 3, and 3.5 m/s. Excessive velocity of air can physically disturb the leaves, causing curling or displacement, which may result in non-uniform drying and compromised quality. Maintaining air velocity within the 2–3 m/s range minimizes these risks, ensuring uniform drying and better retention of sensory and nutritional qualities [22]. Samples (before and after drying) are displayed in **Figure 5**. Mint contains essential oils like menthol, menthone, and 1,8-cineole, which are thermally sensitive. At 35 °C, these compounds evaporate less compared to 50–60 °C drying, resulting in higher retention of aroma and flavor. Studies show up to 30–50% higher essential oil retention at 35 °C than at 50 °C [23]

**Figure 5.** Mint Leaves (a) Before and (b) after Drying

Throughout the experiment, the relative humidity was

maintained at 16%. Weight of dried sample was measured continuously during drying process to find moisture extraction rate. Based on calculated moisture loss, the drying process was terminated once sample weights were reduced to 22 g.

### 3. Calculations

#### 3.1. Energy Balance between the Refrigerant and Airside

Refrigerant properties, such as temperature and pressure at inlet as well as outlet of components, were measured, along with temperature, air velocity, and relative humidity. Energy balance was carried out with the help of **Table 3**. The readings were taken when the DBT and RH of supply air to the dryer were at 30 °C, 35 °C, and 40 °C and RH of around 16%. Energy absorbed by the refrigerant in the evaporators and/or rejected by the desuperheater and sub-cooler can be calculated by equation (1) by knowing mass flow rate of refrigerant and specific enthalpy change across components.

$$\dot{Q} = \dot{m}_{ref} \Delta h \quad (1)$$

The equation (2) calculated power consumed by compressor.

$$\dot{W} = \dot{m}_{ref} \Delta h \quad (2)$$

Where,  $\dot{Q}_R$  is the heat recovered in the desuperheater and sub-cooler, and  $\dot{W}_C$  is power required to run compressor and  $\dot{W}_{auxilliary}$  is total power required for centrifugal fans provided in the system.

The Overall COP (including fan and other system power) and SMER are the two most essential criteria for studying performance of heat pump drying system. COP is described as ratio between heat removed at condenser and power required to run compressor.

**Table 3.** Energy Balance

Parameter	Formula	
Heat gained by air over the desuperheater and sub-cooler coils (kW)	$\rho_{air} \dot{v}_{air} \Delta h_{desuperheater} + \rho_{air} \dot{v}_{air} \Delta h_{subcooler}$	(3)
Heat rejected by refrigerant in the desuperheater and sub-cooler coils (kW)	$\dot{m}_{ref} \Delta h_{desuperheater} + \dot{m}_{ref} \Delta h_{subcooler}$	(4)
Heat rejected by air over the evaporator coils (kW)	$\rho_{air} \dot{v}_{air} \Delta T_{HPE} + \rho_{air} \dot{v}_{air} \Delta T_{LPE(I \ \& \ II)}$	(5)
Heat gained by refrigerant in the evaporator coils (kW)	$\dot{m}_{ref} \Delta h_{HPE+LPEs}$	(6)

Where  $\Delta h$  is the specific enthalpy rise of the refrigerants across the compressors and  $\dot{m}_{ref}$  is mass flow rate of refrigerant, which depends upon volumetric efficiency of compressor for a certain compressor inlet condition.

### 3.2. Drying Characteristics

SMER can be defined as mass of water removed from the drying samples per kW of power supplied for 1hr. to the heat pump systems.

$$SMER = \frac{\dot{m}_w}{\dot{W}_{C(HP)} + \dot{W}_{auxilliary}} \quad (7)$$

The system’s performance is decided by separately evaluating the thermal properties of refrigerant and air. The readings were recorded on both air and refrigerant streams.

Moisture content of sample can be evaluated using equation given below (8):

$$MC_{db} = \frac{M_i - M_d}{M_d} \quad (8)$$

Moisture Ratio (MR) during drying experiment was evaluated by employing equation given below (9):

$$MR = \frac{M - M_e}{M_0 - M_e} \quad (9)$$

Here M represents moisture content,  $M_e$  represents equilibrium moisture content,  $M_0$  denotes initial moisture content. Given high moisture levels in fresh products, Equation (9) can be simplified and expressed as Equation (10):

$$MR = \frac{M}{M_0} \quad (10)$$

Drying rate (DR) of products over-drying experiments can be evaluated using following equation (11).

$$DR = \frac{MC_{t+dt} - MC_t}{dt} \quad (11)$$

During drying, effective moisture diffusivity of mint leaves can be calculated using Fick’s second law of diffusion. This drying behavior is represented mathematically by Equation (12).

$$MR = \frac{8}{\pi^2} \sum_{n=0}^{\infty} \frac{1}{(2n-1)} e^{-\frac{(2n-1)^2 \pi^2 D_{eff} t}{4 L s^2}} \quad (12)$$

For long period, aforementioned equation can be simplified in equation (13).

$$MR = \frac{8}{\pi^2} \exp\left(-\frac{\pi^2 D_{eff} t}{4 L s^2}\right) \quad (13)$$

### 3.3. Color

Color is an important quality parameter of any dried product as it changes during drying due to some biochemical reaction. The color characteristic of dried samples was tested in colorimeter to analyze the amount of color changes ( $\Delta E$ ) (equation 14). Soares et al. [24] used CIE-L\*a\*b\* colorimetric method where L\* estimates whiteness value of a color and ranges from "black-to-white", b\* measures "blue when negative" and "yellow when positive", and a\* measures "green when negative" and "red when positive".

$$\Delta E = \sqrt{(L_0^* - L^*)^2 + (a_0^* - a^*)^2 + (b_0^* - b^*)^2} \quad (14)$$

The chroma index in a colorimeter refers to the saturation or intensity of a color—that is, how vivid or dull the color appears. It is derived from color space models, particularly the CIELAB (L\*a\*b\*) system, and is calculated using a\* (green–red) along with b\* (blue–yellow) coordinates (equation 15):

$$C^* = \sqrt{(a^*)^2 + (b^*)^2} \quad (15)$$

## 4. Results and Discussion

### 4.1. Drying Characteristics

Mint samples initially contained 9.4 g of water per gram of dry matter, which was reduced to 0.23g/g of dry matter after drying. Difference in moisture content on dry and wet basis, as function of drying time, is demonstrated in **Figure 6**. Experimental results showed that increasing air velocity from 2-3m/s actually reduced overall drying time. This improvement is attributed to enhanced mass transfer, as higher airflow increases convective heat transfer rate and decreases thickness of the boundary layer surrounding mint leaves. Consequently, moisture is removed more efficiently from the leaf surface into the surrounding air [25].

**Figure 7** demonstrates variation of moisture ratio against time. Dryer effectively reduced moisture content of mint sample. SMER was high initially, driven by the pressure difference, and decreased moderately over time. The results demonstrate the dryer's efficiency and ability to remove moisture from the material, although some residual moisture remained due to solid bonding forces[26].

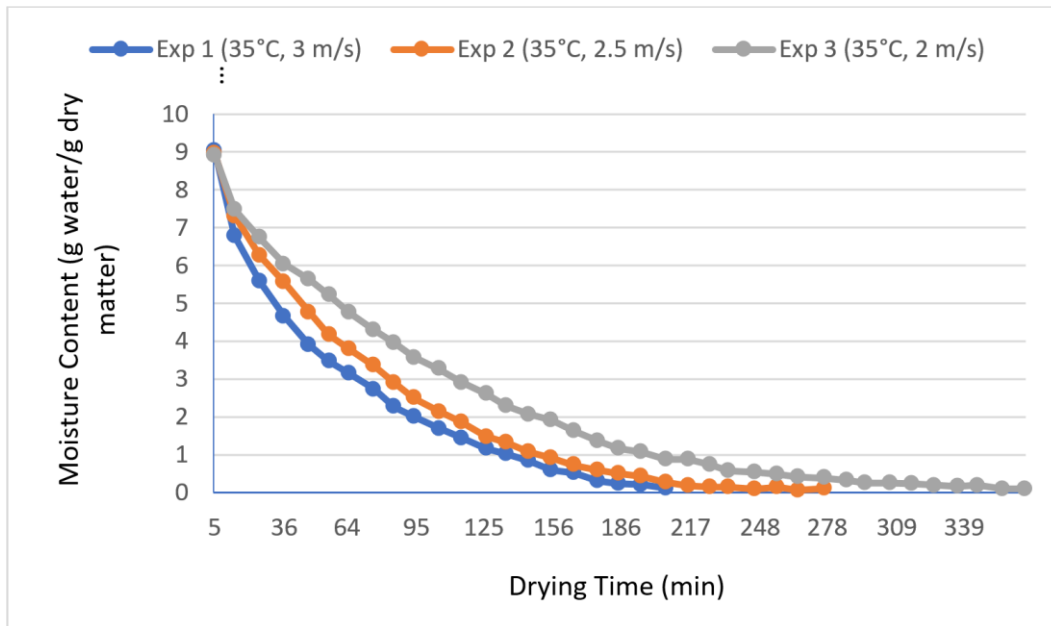
Variation in drying rate has been demonstrated in

**Figure 8.** Higher air velocity corresponds to lower drying time.

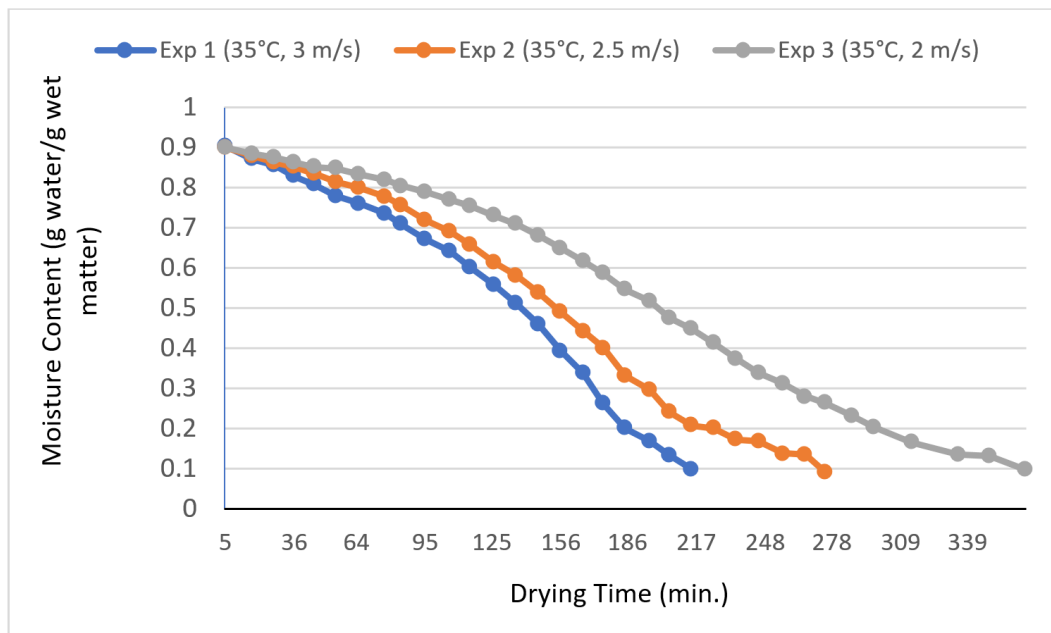
**4.2. Color**

Values of L\* (Lightness), a\*(redness), b\*(yellowness), ΔE (Change in color) and Chroma index are shown in **Table 4**. From the experiments, it is clear that total color change (ΔE) increased from 6.19 at 35 °C to 12.80 at 60 °C, showing that higher temperatures caused noticeable degradation in color. Dried mint leaves at 35 °C exhibited the highest chroma value (C\* = 27.53), reflecting vivid

green coloration. As drying temperature rose from 35 °C to 60 °C, chroma consistently decreased to 23.41, indicating progressive loss of color saturation. The 35 °C drying condition resulted in the lowest ΔE and highest C\* among the dried samples, indicating minimal deviation from the fresh leaf color. Arslan et al. [27] found that drying mint at low temperatures (~35–40 °C) preserves chlorophyll and green coloration better than at higher temperatures. Mint leaves begin to deteriorate and show signs of bursting at temperatures exceeding 35 °C. Therefore, airflows at temperatures above this threshold were intentionally excluded from the experimental conditions.



(a)



(b)

**Figure 6.** Moisture Content Vs. Drying time a) Dry basis b) Wet basis

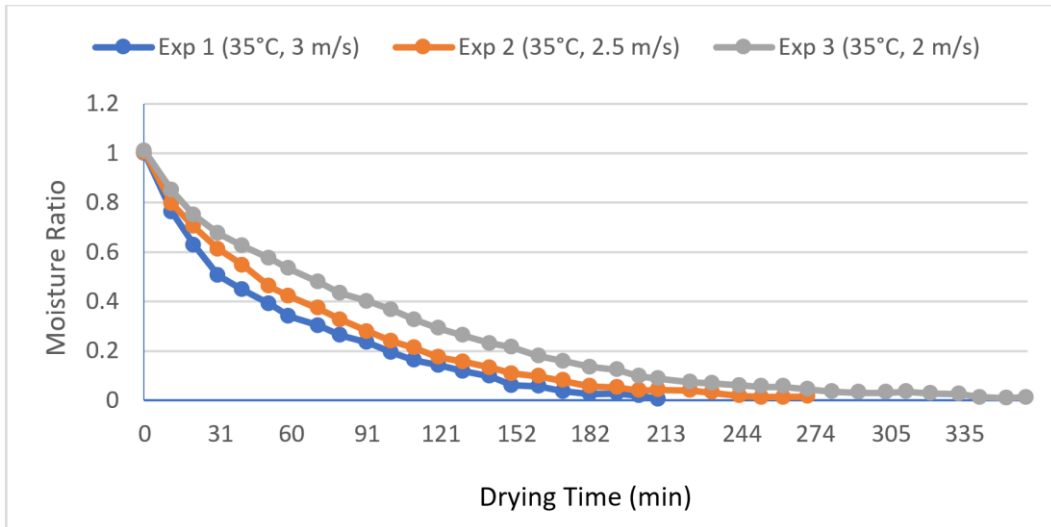


Figure 7. Moisture ratio Vs. drying Time

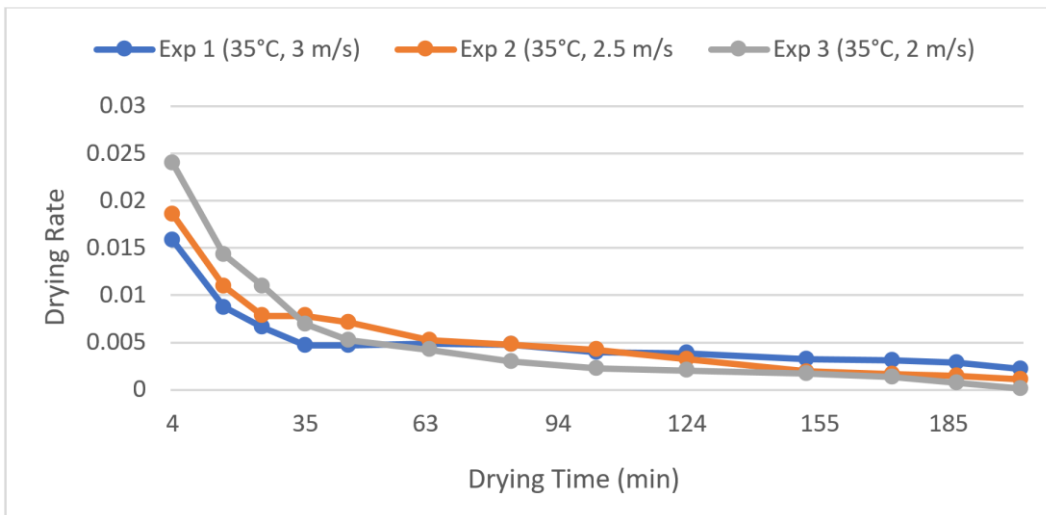


Figure 8. Drying Rate Vs. Drying Time

Table 4. Colour analysis

T (°C)	L*	a*	b*	ΔE	C*
fresh	43.56±0.0597 <sup>a</sup>	-11.89±0.0335 <sup>c</sup>	28.56±0.0571 <sup>b</sup>	---	30.93±0.823 <sup>c</sup>
35	38.62±0.0749 <sup>e</sup>	-9.25±0.0768 <sup>c</sup>	25.93±0.214 <sup>a</sup>	6.18±0.200 <sup>a</sup>	27.53±126 <sup>b</sup>
40	35.16±0.0295 <sup>b</sup>	-8.42±0.0453 <sup>d</sup>	24.35±0.105 <sup>c</sup>	10.01±0.080 <sup>e</sup>	25.76±107 <sup>a</sup>
45	35.1±0.0245 <sup>c</sup>	-8.21±0.0253 <sup>e</sup>	23.94±0.205 <sup>b</sup>	10.31±0.007 <sup>b</sup>	25.30±145 <sup>e</sup>
50	34.15±0.0362 <sup>d</sup>	-7.59±0.035 <sup>a</sup>	23.01±0.211 <sup>c</sup>	11.74±0.0125 <sup>b</sup>	24.22±124 <sup>b</sup>
60	33.45±0.0232 <sup>a</sup>	-7.18±0.0252 <sup>b</sup>	22.28±0.125 <sup>e</sup>	12.79±0.0144 <sup>d</sup>	23.40±156 <sup>a</sup>

Different letters in the columns have a significant difference at the 1% probability level.

### 4.3. Heat Pump Performance

The drying cycles reveal an initial increase in overall energy consumption, attributed to the thermal inertia of the system. As drying process progresses, evaporator's heat absorption from moisture-laden air intensifies, resulting in an elevated cooling load[28]. To counteract this increased

load, expansion valve modulates refrigerant flow, necessitating compressor to operate at a higher capacity. Consequently, the power consumption escalates, exacerbated by higher supply air velocities, which also augment fan power consumption. The power consumption Vs. Time is shown in **Figure 9**.

**Table 5** shows some important parameters in evaluating the drying efficiency of a dryer: drying time, coefficient of performance, total energy consumption, and airflow velocity. Retention of volatile compounds in mint leaves can be enhanced by increasing air velocities as rapid removal of moisture minimises the thermal degradation of sensitive compounds but higher velocities contribute to power consumption. In this study, the air velocities from 2-3 m/s were selected. Drying time increases as air velocity decreases. Total energy consumption decreases as air velocity decreases. COP overall and COP<sub>HP</sub> decrease as air velocity decreases. SMER decreases as air velocity decreases.

The findings indicate that a decrease in air velocity extends the drying duration and results in reduced energy usage and overall efficiency (both COP overall and COP<sub>HP</sub>). However, this is accompanied by a decline in

SMER, suggesting that effectiveness of drying process diminishes at lower air velocities. The purpose of using a high-pressure evaporator separately in the air path is to cool return air from dryer to dew point temperature to effectively utilize surface of the LPE for latent heat recovery of return air [29]. According to Chua et al. [17], 35% extra heat can be reclaimed using a multistage evaporator setup. Enhancing heat recovery primarily involves raising ratio of latent heat to total heat load at evaporators. To analyse this, experiments were conducted using a single-stage vapor compression system, focusing on variations in drying temperature and humidity at dryer's inlet. During tests, both refrigerant pressure and mass flow rate via high-pressure evaporator (HPE) were maintained constant, along with a fixed air volume flow rate. The variation in relative humidity and supply temperature is shown in **Figure 10**.

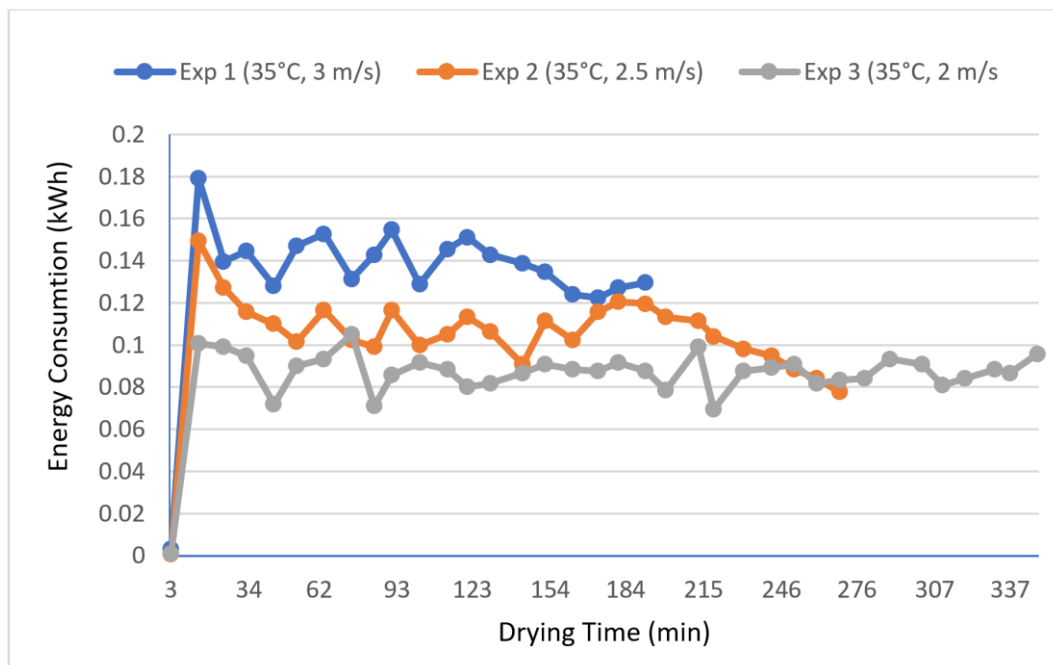


**Figure 9.** Energy Consumption Vs Drying Time

**Table 5.** Experimental results

	Experiment 1	Experiment 2	Experiment 3
Total energy consumption (kWh)	3.5	3.2	3.158
Drying air temperature ( °C)	35	35	35
Drying Time (hrs)	3.5	4	4.5
Flow rate (m <sup>3</sup> /h)	900	800	700
Air velocity (m/s)	3	2.5	2
COP overall	2.54	2.35	2.15
COP <sub>HP</sub>	5.06	4.85	4.5
SMER	0.92	0.83	0.79

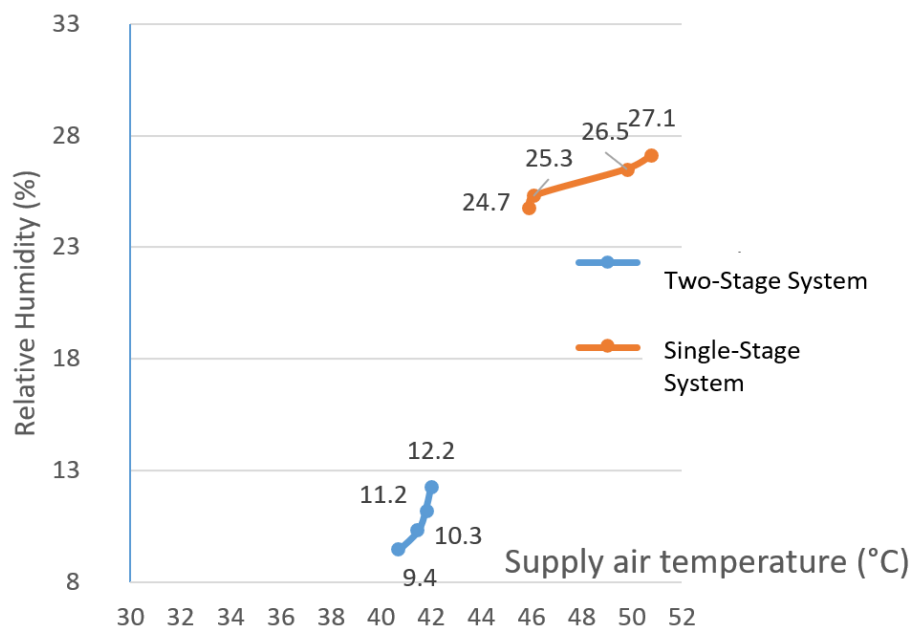


Figure 10. Effect of single-stage and two-stage systems on RH

## 5. Conclusions

This experimental investigation demonstrated the efficacy of two-stage heat pump drying system for drying mint leaves at low-temperature. The system's innovative defrosting arrangement ensured uninterrupted air supply, thereby maintaining a consistent drying process. Findings revealed a significant decline in drying time with elevated air velocity, accompanied by a high SMER of 0.84 kg/kW-hr. Increasing air velocity from 2 to 3m/s significantly decreased drying time due to improved convective heat as well as mass transfer, although it also led to higher energy consumption and reduced COP. Although the overall energy consumption increased with drying time, the system achieved a remarkable average COP of 4.8, indicating high energy efficiency. Among all conditions tested, drying at 35 °C with air velocity of 3m/s provided best balance between drying efficiency and color preservation, with lowest total color change ( $\Delta E$ ) and highest chroma ( $C^*$ ), indicating minimal degradation of leaf quality. These results suggest that low-temperature drying is optimal for maintaining the visual and potential nutritional quality of mint. This low-temperature heat pump drying system offers a viable alternative to conventional drying methods, enabling production of high-quality dried products while minimizing energy consumption.

## Acknowledgments

The authors express appreciation to Panasia Engineers Pvt—Ltd; Navi Mumbai, Maharashtra, India, for providing its research laboratory for experiments.

## Funding Sources

Authors acknowledge financial support received from Institute of Chemical Technology, Mumbai, Maharashtra, India, 400019.

## Declaration of Competing Interest

Authors state that there are no financial or personal relationships that could have influenced the outcomes or interpretation of the research presented in this article.

## Nomenclature

COP: Coefficient of performance  
 $C_p$ : Specific heat capacity [kJ/kg °C]  
 $C$ : Chroma Index  
 DB: Dry Basis  
 DBT: Dry Bulb Temperature  
 $H$ : Specific enthalpy [kJ/kg]  
 HP: High-pressure system  
 HPD: Heat pump Dryer  
 HPE: High-pressure evaporator  
 HRR: Heat rejection rate  
 $\dot{Q}$ : Heat transfer [kW]  
 LPE: Low-pressure evaporator  
 LP: Low-pressure system  
 RH: Relative humidity  
 SMER: Specific moisture extraction rate  
 TXV: Thermostatic expansion valve  
 $W$ : Work transfer rate [kW]  
 WB: Wet Basis  
 WBT: Wet Bulb Temperature

## Subscripts

R: Rejected  
 A: Air  
 W: Water  
 Ref: Refrigerant  
 C: Compressor  
 Sat: Saturation

## REFERENCES

- [1] M. Aghbashlo, S. Hosseinpour, and A. S. Mujumdar, "Application of Artificial Neural Networks (ANNs) in Drying Technology: A Comprehensive Review," *Drying Technology*, vol. 33, no. 12, pp. 1397–1462, 2015, doi: 10.1080/07373937.2015.1036288.
- [2] V. Minea, "Drying heat pumps-Part II: Agro-food, biological and wood products," *International Journal of Refrigeration*, vol. 36, no. 3, pp. 659–673, 2013, doi: 10.1016/j.ijrefrig.2012.11.026.
- [3] N. Colak and A. Hepbasli, "A review of heat pump drying: Part 1 - Systems, models and studies," *Energy Convers Manag*, vol. 50, no. 9, pp. 2180–2186, 2009, doi: 10.1016/j.enconman.2009.04.031.
- [4] M. Mohanraj, Y. Belyayev, S. Jayaraj, and A. Kaltayev, "Research and developments on solar assisted compression heat pump systems – A comprehensive review (Part A: Modeling and modifications)," *Renewable and Sustainable Energy Reviews*, vol. 83, no. July 2016, pp. 90–123, 2018, doi: 10.1016/j.rser.2017.08.022.
- [5] C. Ertekin and N. Heybeli, "Thin-layer infrared drying of mint leaves," *J Food Process Preserv*, vol. 38, no. 4, pp. 1480–1490, 2014, doi: 10.1111/jfpp.12107.
- [6] J. Szadzi, S. J. Kowalski, and J. M. Ł., "Chemical Engineering and Processing: Process Intensi fication Microwave- and infrared-assisted convective drying of green pepper: Quality and energy considerations," vol. 98, pp. 155–164, 2015, doi: 10.1016/j.cep.2015.10.001.
- [7] J. Yongsawatdigul and S. Gunasekaran, "Microwave-vacuum drying of cranberries: Part I. Energy use and efficiency," *J Food Process Preserv*, vol. 20, no. 2, pp. 121–143, 1996, doi: 10.1111/j.1745-4549.1996.tb00850.x.
- [8] F. Lüle and T. Koyuncu, "Convective and Microwave Drying Characteristics of Sorbus Fruits ( Sorbus domestica L. )," *Procedia Soc Behav Sci*, vol. 195, pp. 2634–2643, 2015, doi: 10.1016/j.sbspro.2015.06.467.
- [9] M. A. Hossain, K. Gottschalk, and M. S. Hassan, "Mathematical model for a heat pump dryer for aromatic plant," *Procedia Eng*, vol. 56, pp. 510–520, 2013, doi: 10.1016/j.proeng.2013.03.154.
- [10] M. N. A. Hawlader, C. O. Perera, and M. Tian, "Properties of modified atmosphere heat pump dried foods," *J Food Eng*, vol. 74, no. 3, pp. 392–401, 2006, doi: 10.1016/j.foodeng.2005.03.028.
- [11] Y. Potisate and S. Phoungchandang, "Chlorophyll retention and drying characteristics of ivy gourd leaf (coccinia grandis voigt) using tray and heat pump-assisted dehumidified air drying," *Drying Technology*, vol. 28, no. 6, pp. 786–797, 2010, doi: 10.1080/07373937.2010.482698.
- [12] K. Rayaguru and W. Routray, "Effect of drying conditions on drying kinetics and quality of aromatic Pandanus amaryllifolius leaves," *J Food Sci Technol*, vol. 47, no. 6, pp. 668–673, 2010, doi: 10.1007/s13197-010-0114-1.
- [13] B. R. TOAL., R. MORGAN, and M. J. T., "Experimental Studies of Low-Temperature Drying By," *Int J Energy Res*, vol. 12, no. September 1986, pp. 315–344, 1988.
- [14] V. Sosle, G. S. V. Raghavan, and R. Kittler, "Low-temperature drying using a versatile heat pump dehumidifier," *Drying Technology*, vol. 21, no. 3, pp. 539–554, 2003, doi: 10.1081/DRT-120018461.
- [15] G. Angelino and C. Invernizzi, "General method for the thermodynamic evaluation of heat pump working fluids," *International Journal of Refrigeration*, vol. 11, no. 1, pp. 16–25, 1988, doi: 10.1016/0140-7007(88)90007-2.
- [16] Praphanpong Somsila, Eakpoom Boonthum, and Songsupa Pumchumpol, "View of Performance Enhancement of Heat Pump Dryer using Heat Recovery," *Journal of Advanced Research in Fluid Mechanics and Thermal Sciences*, vol. 118, no. 2, pp. 34–46, Jun. 2024, doi: 10.37934/arfmts.118.2.3446.
- [17] K. J. Chua and S. K. Chou, "A modular approach to study the performance of a two-stage heat pump system for drying," *Appl Therm Eng*, vol. 25, no. 8–9, pp. 1363–1379, 2005, doi: 10.1016/j.applthermaleng.2004.08.012.
- [18] C. J. Li and C. C. Su, "Experimental study of a series-connected two-evaporator refrigerating system with propane (R-290) as the refrigerant," *Appl Therm Eng*, vol. 23, no. 12, pp. 1503–1514, 2003, doi: 10.1016/S1359-4311(03)00082-6.
- [19] A. Du and J. Long, "Heating performance of a novel two-stage evaporator air-source heat-pump for drying applications," *Drying Technology*, vol. 40, no. 7, pp. 1356–1368, 2022, doi: 10.1080/07373937.2020.1869036.
- [20] W. T. Simpson, "Effect of air velocity on the drying rate of single eastern white pine boards," *Research Note - Forest Products Laboratory, USDA Forest Service*, no. FPL-RN-266, pp. 5 pp.-5 pp., 1997.
- [21] Y. Chung, J. W. Yoo, G. T. Kim, and M. S. Kim, "Prediction of the frost growth and performance change of air source heat pump system under various frosting conditions," *Appl Therm Eng*, vol. 147, no. October 2018, pp. 410–420, 2019, doi: 10.1016/j.applthermaleng.2018.10.085.
- [22] M. Fatouh, M. N. Metwally, A. B. Helali, and M. H. Shedid, "Herbs drying using a heat pump dryer," *Energy Convers Manag*, vol. 47, no. 15–16, pp. 2629–2643, Sep. 2006, doi: 10.1016/j.enconman.2005.10.022.
- [23] M. C. S. G. Blanco, L. C. Ming, M. O. M. Marques, and O. A. Bovi, "Drying Temperature Effects in Peppermint Essential Oil Content and Composition," *Acta Horti*. 569, pp. 95–98, Feb. 2002. doi: 10.17660/ActaHortic.2002.569.15.

- [24] L. Soares and A. Alves, "Analysis of colorimetry using the CIE-L\*a\*b\* system and the photocatalytic activity of photochromic films," *Mater Res Bull*, vol. 105, pp. 318–321, Sep. 2018, doi: 10.1016/j.materresbull.2018.05.012.
- [25] A. K. Babu, G. Kumaresan, V. Antony Aroul Raj, and R. Velraj, "Experimental Investigations of Thin-layer Drying of Leaves in a Heat-Pump Assisted Tray-type Batch Drying Chamber," *Strojnicki Vestnik/Journal of Mechanical Engineering*, vol. 66, no. 4, pp. 254–265, 2020, doi: 10.5545/sv-jme.2019.6510.
- [26] A. Salazar-Hincapié, A. Delgado-Mejía, A. F. Romero-Maya, and E. Duque-Grisales, "Experimental assessment of the thermal performance of a heat pump dryer system based on the variations in compressor discharge pressure on oregano drying," *Energies (Basel)*, vol. 13, no. 23, Dec. 2020, doi: 10.3390/en13236333.
- [27] D. Arslan, M. M. Özcan, and H. O. Mengeş, "Evaluation of drying methods with respect to drying parameters, some nutritional and colour characteristics of peppermint (*Mentha x piperita* L.)," *Energy Convers Manag*, vol. 51, no. 12, pp. 2769–2775, Dec. 2010, doi: 10.1016/j.enconman.2010.06.013.
- [28] A. M. Alsayah, J. J. Faraj, and A. A. Eidan, "The augmentation of the heat recovery by using evaporative cooling in HVAC applications: Experimental study," *International Journal of Thermofluids*, vol. 22, May 2024, doi: 10.1016/j.ijft.2024.100671.
- [29] A. Cichoń and W. Worek, "Analytical investigation of a novel system for combined dew point cooling and water recovery," *Applied Sciences (Switzerland)*, vol. 11, no. 4, pp. 1–18, Feb. 2021, doi: 10.3390/app11041481.